Calibration free distortion correction for propeller EPI

S. Skare[1], J. Andersson[2], and R. Bammer[1]

[1]Radiology, Stanford University, Palo Alto, CA, United States, [2]FMRIB, Oxford University, Oxford, United Kingdom

Introduction We have shown earlier that the SAP-EPI pulse sequence [1] can reduce geometric distortions in high-resolution DWI. When combined with GRAPPA (*R*=3), distortion reductions of up to one order of magnitude have been achieved [2]. Being a pseudo non-Cartesian technique, the minor distortions that remain in the blade data give rise to minor blurring (or local swirls) in the image. In this work, we present a distortion correction method tailored for SAP-EPI data that corrects the acquired blades images in a fast iterative manner prior to gridding. This algorithm is based on formalism in unpublished work by Andersson et al. [3], using a generalization of the reversed gradient polarity method, 'RGPM' [4]. The main difference being the estimation of *one* common distortion field for an arbitrary number of images distorted in different directions and magnitudes. Demonstration of the correction efficiency for SAP-EPI on a phantom and DTI brain data on a volunteer is provided.

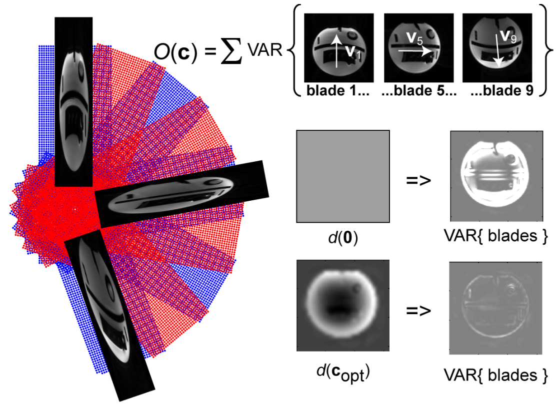

Figure 1. Distortion correction procedure. A distortion field, $d(\mathbf{c})$, is found by minimizing the cost function, $O(\mathbf{c})$. Variance maps over blades before and after correction shown to the bottom-right.

Materials & Methods SAP-EPI phantom data was acquired on a GE 3T Excite scanner equipped with 40 mT/m gradients and an 8-channel RF coil (Invivo corporation, Peewaukee, WI). GRAPPA factors of *R*=1-3 were used with nine Half-Fourier blades of size 64x160 (freq. x phase) swept over 0-160°, yielding a final image resolution of 288x288. Other parameters were; TE/TR=23/4000 ms, FOV=26 cm, and slice thickness=5 mm. In addition, DTI-SAP-EPI brain data was acquired on a GE 1.5T Excite system using 2 *b*=0 and 13 diffusion directions (*b*=1000 s/mm^2), *R*=2, and six 64x256 blades covering 0-150°. The distortion field was estimated on the first *b*=0 image and applied to the remaining data set. As a key pre-processing step in the correction, each blade was zerofilled in *k*-space along the k_x direction, Fourier transformed, and counter-rotated by its nominal blade angle, making *N* temporary blade images, $I_{1..N}$, of the same size and patient orientation, each of which is distorted along a unique direction, $\mathbf{v}_j$. A corrected blade, f_j, is obtained by resampling I_j based on the distortion field $d(\mathbf{c})$ along the direction $\mathbf{v}_j$, and intensity modulated according to

$$f_j = I_j(d(\mathbf{c})\mathbf{v}_j)\left(1 + D_{\mathbf{v}j}(d(\mathbf{c}))\right) \qquad [1]$$

where $D_{\mathbf{v}j}(d(\mathbf{c}))$ denotes the directional derivative of $d(\mathbf{c})$ along $\mathbf{v}_j$. To find a suitable $d(\mathbf{c})$, a cost function, minimizing the difference between the blade images was defined as:

$$O(\mathbf{c}) = \sum_{\mathbf{x}\in V}\left(\frac{1}{N-1}\sum_{j=1}^{N}\left(\frac{1}{N}\sum_{k=1}^{N} f_k - f_j\right)^2\right) \qquad [2]$$

While not shown here, the analytical derivatives of $O(\mathbf{c})$ w.r.t. each member in **c**, was derived, which allowed for the use of a fast derivative based search algorithm (quasi-Newton).

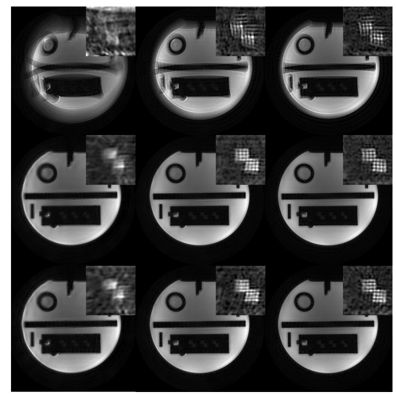

Figure 2. SAP-EPI with GRAPPA R=1-3 (left to right) using nine 64x288 blades at 3T. Top: Before correction. Mid: After correction. Bottom: After correction using only every other blade

Results In Fig. 1 the blade images for the *R*=1 phantom scan is shown on top of the propeller blades. The corresponding zerofilled and counter-rotated blades are shown above with white arrows indicating their individual distortion direction. Below, the variance maps before (top) and after (bottom) correction is given in conjunction with the corresponding $d(\mathbf{c})$. Fig. 2 shows the gridded phantom data acquired with *R*=1-3 (left to right). The rows show the data without correction (top), with correction (middle) and finally with correction and gridding using only five of the nine blades (bottom). Similar performance is seen for nine and five blades for all reduction factors. *R*=2 and 3 renders a sharper image than *R*=1, signifying the necessity of reducing the distortion levels in the acquisition in addition to post-processing. Fig. 3 shows *b*=1000 s/mm^2 (isotropic) images on the volunteer data before (left) and after (right) distortion correction.

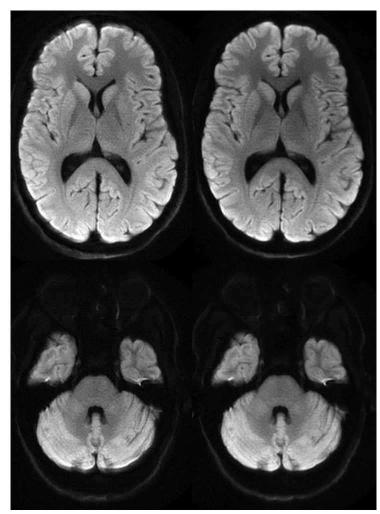

Figure 3 Isotropic DW images before (left) and after (right) correction

Discussion & Conclusion A distortion correction algorithm tailored for SAP-EPI data has shown to correct for geometric distortions using only the blades needed for the image formation. For a DTI scan like in Fig. 3, the estimation needs only to be performed once and then applied to the remaining dataset. To further reduce the estimation time (currently a few mins) a subset of blades may be used during the iteration process. Moreover, the blade resolution may be decreased for the same purpose, since $d(\mathbf{c})$ is parameterized. Important to note is that there is an upper distortion limit beyond which the data cannot be corrected by post-processing even if the true ΔB_0 field is known exactly. To prevent this, the GRAPPA reduction factor can be increased and the blade width decreased. Furthermore, we recently proposed the use of a DW-SAP-EPI sequence with *dual* orthogonal blade readouts to shorten the scan time [5]. Since the two readouts will have slightly different image contrast due to TE differences, Eq. 2 will be modified to first take the variance of the blades belonging to each readout separately and then summed together. Finally, we have observed that Nyquist ghosts present in oblique blade data can mislead the algorithm. To avoid this, phase encoding blip compensation gradients will be added in the SAP-EPI sequence.

References [1] Skare S *et al.* Magn Reson Med 2006;55(6):1298-1307. [2] Skare S. 2006; Seattle. ISMRM. p 857. [3] Andersson J, Miller K. Personal Communication 2007. [4] Chang H, Fitzpatrick J. IEEE Trans Med 1992;11:319–329. [5] Skare S *et al.*; 2007; ISMRM Workhop on Non-Cartesian Imaging, Sedona.

Acknowledgements This work was supported in part by the NIH (2R01EB002711, 1R21EB006860, and P41RR09784), Swedish Research Council (K2007-53P-20322-01-4), the Lucas foundation, and the Oak foundation.